Hollow Cathode Plasma Synthesis of Carbon Nanofiber Arrays at Low Temperature

Andrzej Huczko,* Hubert Lange, and Maciej Sioda

Department of Chemistry, Warsaw University, 02-093 Warsaw, Poland

Yan Qiu Zhu, Wen Kuang Hsu, Harold W. Kroto, and David R. M. Walton

School of Chemistry, Physics and Environmental Science, University of Sussex, Brighton BN1 9QJ, U.K.

Received: October 1, 2001; In Final Form: November 28, 2001

Aligned carbon nanofibers/tubes, ca. 20−50 nm in diameter, were generated by hollow cathode glow discharge decomposition of $Fe(C_5H_5)_2$ in He at ca. 200 °C on an Al_2O_3 membrane. The as-deposited product consists of bundles of amorphous carbon nanofibers with numerous Fe nanoparticles embedded therein. Heating at 1100 °C under Ar produced well-crystallized carbon nanotubes.

Since their discovery[1,2] and successful large scale production,[2,3] research into carbon nanotubes has developed rapidly. Such nanotubes exhibit a wide range of interesting properties, including field emission with very low turn-on field, as well as excellent coherent monochromatic electron beams. The coherence of the emitted electrons is considerably greater than that produced by a standard tungsten point source. This fact may prove to be very useful in electronics, for example, the nanotubes may be used as cold cathodes for flat panel and holographic displays. Indeed, the first prototype has already been reported.[4] To date, techniques developed to produce nanostructures include laser ablation, arc-discharge, and chemical vapor deposition (CVD). However, these methods involve high temperatures,[2,3,5,6] with the result that carbon nanotube characterization and applications have been hampered because of the uncontrollable morphology and orientation that occurs when condensed nanotubes are grown in the gas phase. Recent studies have shown that the direction of growth and the morphologies of carbon nanotubes can be tailored systematically by selecting various templates (e.g., anodic aluminum oxide, AAO, and track membranes).[7] Template-based methods for producing polymers, metals, semiconductors, and other materials have been reviewed,[8] and the generation of aligned carbon nanotubes in particular has been described.[9] The CVD technique successfully produces aligned tubular nanostructured carpets at medium temperatures (600−1200 °C). However, lower temperatures are still needed if nanotubes are to be made successfully for electronic applications and integrated microelectronics.[5,10] Thus, reduction of the growth temperature below 600 °C, which is acceptable for field emission display (FED) construction using a glass substrate,[8,11] is of great interest.

Plasma deposition for carbon nanotube production has recently attracted much attention because of its effective growth at low temperatures.[10] Nonequilibrium plasma discharges generate large quantities of reactive species, suitable for various chemical transformations.[12] Electronic excitation possesses advantages over thermal and photon activation, which permit operation at "effective" ambient temperatures. In fact, plasma processes have been widely used in microelectronics, especially for thin film production.[13] Recently, hollow cathode glow discharges (HCGD) have been employed to deposit hydrogenated CN_x films[14] and amorphous carbon (*a*-C:H) layers[15] and to evaporate materials.[16]

Previously, we reported the deposition of carbon on an AAO template using a dielectric barrier discharge plasma in various hydrocarbons.[17] We now describe the generation of carbon nanofibers perpendicular to the AAO substrate by using a hollow (graphite) cathode discharge CVD technique. Upon heat treatment, these fibers are converted into well-crystallized carbon nanotubes.

The equipment (Figure 1) consists of a HCGD plasma source and a downstream region where substrates are positioned. An AAO membrane ($10 \times 4 \times 0.06$ mm^3) and $Fe(C_5H_5)_2$ (20 mg) were placed inside the hollow graphite cathode (40 mm long, 5 mm i.d.) and anode, respectively. The construction of the reactor allowed us to locate the substrate either perpendicular or parallel to the discharge channel. A He flow (0.67 kPa; 0.2 cm^3 s^{-1} STP) enabled transport of $Fe(C_5H_5)_2$ vapor to the deposition zone. The $Fe(C_5H_5)_2$ flow during discharge (averaged over time from the mass decrease) was ca. 0.4 mg min^{-1}. After a 30 min discharge, the cathode wall temperature was raised from room temperature to ca. 90 °C (thermocouple measurement). The discharge current and cathode−anode voltage drop were 60 mA and 380 V, respectively.

During discharge, the spectroscopic features of the plasma were monitored optically.[18] An ST8 CCD camera, coupled to a high-resolution spectrograph, was used to identify the atomic lines and molecular bands. The results confirmed partial dissociation of $Fe(C_5H_5)_2$ into radicals and atomic species in the plasma zone. The typical atomic emission lines, He (388.8 nm), Fe (516.7 nm), H (656.2 nm), and C (247.8 nm), were identified.

The strongest bands were those emitted by C_2 ($d\ ^3\Pi_g \rightarrow a\ ^3\Pi_u$, e.g., 517 nm) and CH ($A\ ^2\Delta \rightarrow X\ ^2\Pi$, 432 nm) radicals. Weak bands, for example, CO ($B\ ^1\Sigma \rightarrow A\ ^1\Pi$, e.g., 520 nm) and CN ($B\ ^2\Sigma^+ \rightarrow X\ ^2\Sigma^+$, e.g., 388 nm), were also observed. Figure 2 summarizes the detected band systems. The well-known violet CN band was used to determine the plasma temperature applying the Boltzmann plot method by resolving the rotational structure of the P(0,0) branch. Our results showed that the average temperature in the discharge zone was 200 ± 15 °C.

* To whom correspondence should be addressed. E-mail: ahuczko@chem.uw.edu.pl.

10.1021/jp013669g CCC: $22.00
Published on Web 01/26/2002

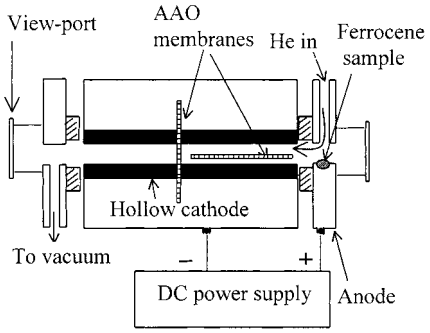

Figure 1. HCGD system.

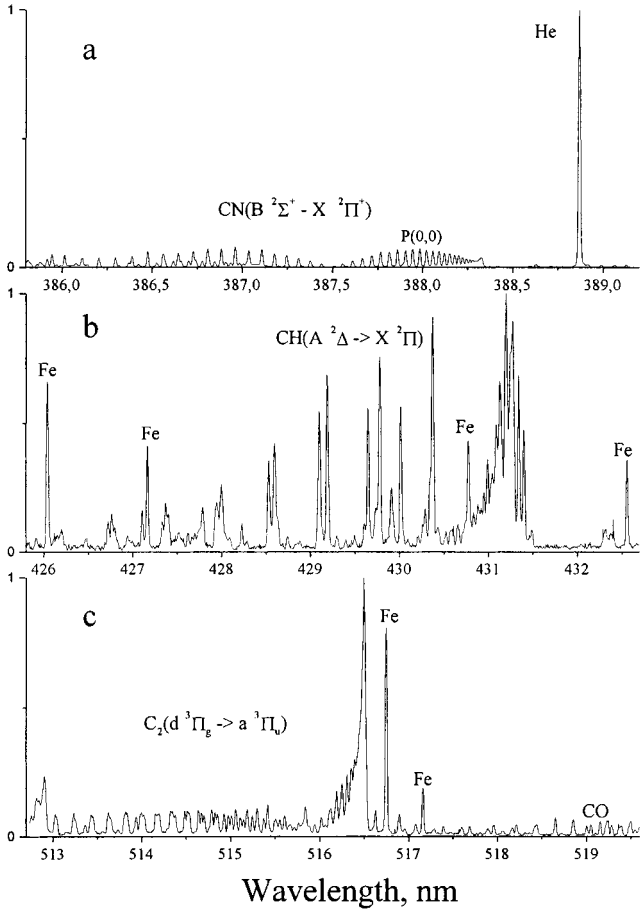

Figure 2. Molecular bands and atomic lines spectra of HCGD in a He−Fe(C_5H_5)$_2$ mixture: (a) CN (388.3 nm), He (388.8 nm); (b) CH (431.4 nm), Fe (432.5, 430.7, 427.1, 426.0 nm); (c) C_2 (516.5 nm), CO (519.8 nm), Fe (516.7, 517.1 nm).

The resulting dark film, deposited on the surface of the AAO membrane positioned parallel to the cathode axis, was examined by scanning electron microscopy (SEM, Leo 5000, operated at 20 keV). The sample was subjected to ultrasonic treatment in acetone for 30 min and then transferred to a Cu grid coated with a holey carbon film for transmission electron microscopic investigations (TEM, H-7100, operated at 100 keV and CM200 with an energy dispersive x-ray (EDX) equipment attachment operated at 200 keV). Other as-grown samples were heated to 1100 °C for 5 h under an Ar flow. After cooling, they were again treated in acetone in an ultrasonic bath for 3 h, prior to transfer to the Cu grid for TEM examination.

SEM showed that the as-grown black sample consisted of flat carpet-like films with a uniform "pile" and irregular microscopic surface cracks (Figure 3a, bottom view). The overall

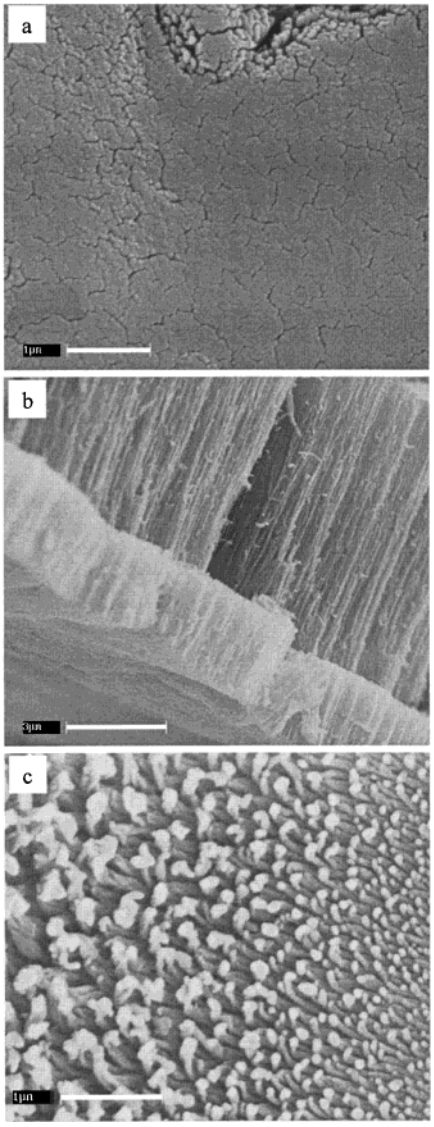

Figure 3. SEM images of aligned nanofibers: (a) bottom view; (b) side view; (c) top view.

size of the film was approximately that of the substrate, that is, $10 \times 4 \times 0.06$ mm^3. The film, ca. 3−10 μm thick, comprised well-aligned nanofiber bundles (Figure 3b, side view). It is noteworthy that these bundles were very homogeneous and contained few nanoparticles. The nanofibers were ca. 20−50 nm in diameter and exhibited no direct relationship to the AAO channel structural parameters. At the fiber tips, white particles were apparent, presumably consisting of coalesced Fe particles as a result of Fe(C_5H_5)$_2$ decomposition (Figure 3c, top view).

TEM showed that the resulting nanofibers were relatively straight and uniform, displaying dimensions similar to those observed by SEM (Figure 4a). At higher magnification, the fibers appeared to be amorphous, with numerous tiny dark particles uniformly distributed throughout (Figure 4b). Hollow cores were absent. EDX analysis showed that the fibers consisted solely of C and Fe. Thus, the samples were made up of aligned bundles of amorphous carbon nanofibers, with Fe particles embedded therein. Very few Fe particles were attached to the fiber tips, in contrast to the SEM observation (Figure 3c). We deduce therefore that ultrasonic treatment has removed the majority of the particles from the fiber tips.

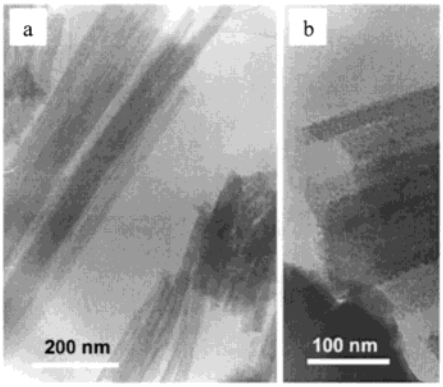

Figure 4. TEM images of the nanofibers: (a) bundles of nanofibers; (b) at higher magnification the embedded Fe particles are apparent (tiny dark spots).

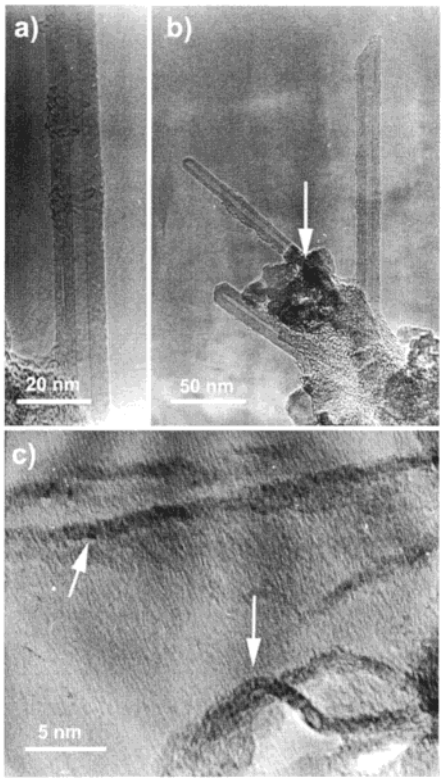

Figure 5. HRTEM images: (a) well-crystallized carbon nanotube; (b) nanotubes and Fe slabs (arrowed); (c) buckled and twisted nanotubes (arrowed).

After heat treatment (1100 °C, 5 h), further HRTEM observations showed that the amorphous fibers had been converted into well-crystallized nanotubes (Figure 5a,b): uniform, straight, and analogous to those produced by arc-discharge methods. In some cases, the nanotubes were buckled and twisted, presumably as a result of the 3 h ultrasonic treatment, which caused some of the poorly crystallized tubes to disintegrate (Figure 5c, arrowed). It is interesting to note that we failed to detect any Fe particles or encapsulates in the nanotubes; however, large slab-like Fe particles, located in the carbonaceous phases (Figure 5b, arrowed), were detected by EDX. This indicates that long-distance migration of Fe and C atoms had occurred during the carbon nanotube graphitization process. At this stage, it is not at all clear how the Fe influences the carbon graphitization and nanotube formation during heat treatment. However, a catalytic effect is expected, as occurred in the $Fe(C_5H_5)_2$ pyrolysis step (temperature > 600 C°) for carbon nanotube formation.[19]

The HCGD process involves plasma pyrolysis of $Fe(C_5H_5)_2$ in a He/C atmosphere. The advantages of this single-step approach include the following: (1) the absence of a prepatterned catalytic substrate, (2) low deposition temperature, (3) high deposition rate, and (4) simple equipment. Emission spectroscopic analysis of the plasma zone revealed the predominance of C_2 radicals, which are believed to constitute the key intermediate phase in nanomaterial formation. Previous carbon isotope distribution studies[20] provided evidence for the presence of C_n ($n < 3$) species in the carbon plasma and for the formation of carbon nanostructures as a result of the collision of small C_n species. Xia et al.[21] have reported extensive molecular dynamic simulations of single-walled carbon nanotube growth as a result of adding C_2 species to the open-ended nanotube tips at 1000−3500 K in the absence of catalyst. In this context, the plasma-generated C_2 species, together with the catalytic Fe, give rise to nanofibers at fairly low "effective" temperatures (ca. 200 °C).

In summary, we have demonstrated that the HCGD process offers great potential for generating aligned carbon nanofibers at low temperature. Well-aligned and perpendicular to the substrate carbon nanofibers have been synthesized by plasma-induced decomposition of $Fe(C_5H_5)_2$ at 200 °C on an AAO membrane. After further heat treatment, well-crystallized carbon nanotubes (ca. 20−50 nm diam, straight and uniform) were generated.

Acknowledgment. The work was supported by the Committee for Scientific Research (KBN) through the Department of Chemistry, Warsaw University, under Grant No. 3 T09A 058 16, the Royal Society, and the Leverhulme Trust.

References and Notes

(1) Endo, M. *CHEMTECH* **1988**, *18*, 568.
(2) Iijima, S. *Nature (London)* **1991**, *354*, 56.
(3) Ebbesen, T. W.; Ajayan, P. M. *Nature (London)* **1992**, *358*, 220.
(4) Murakami, H.; Hirakawa, M.; Tanaka, C.; Yamakawa, H. *Appl. Phys. Lett.* **2000**, *76*, 1776.
(5) Journet, C.; Bernier, P. *Appl. Phys. A* **1998**, *67*, 1.
(6) Smalley, R. E. *Mater. Sci. Eng., B* **1993**, *19*, 1.
(7) Martin, C. R. *Science* **1994**, *266*, 1961.
(8) Huczko, A. *Appl. Phys. A* **2000**, *70*, 365.
(9) Huczko, A. *Appl. Phys. A* **2001**, *73*, 1.
(10) Merkulov, V. I.; Lowndes, D. H.; Wei, Y. Y.; Eres, G.; Voelkl, E. *Appl. Phys. Lett.* **2000**, *76*, 3555.
(11) Okai, M.; Muneyoshi, T.; Yaguchi, T.; Sasaki, S. *Appl. Phys. Lett.* **2000**, *77*, 3468.
(12) Falkenstein, Z. *J. Appl. Phys.* **1999**, *85*, 525.
(13) Caquineau, H.; Despax, B. *Recent Res. Dev. Vacuum Sci. Tech.* **2000**, *2*, 1.
(14) Balaceanu, M.; Grigore, E.; Truica-Marasescu, F.; Pantelica, D.; Negoita, F.; Pavelescu, G.; Ionescu, F. *Nucl. Instrum. Methods Phys. Res., Sect. B* **2000**, *161*−*163*, 1002.
(15) Buuron, A.; Koch, F.; Nöthe, M.; Bolt, H. *Surf. Coat. Technol.* **1999**, *116*−*119*, 755.
(16) Rohrbach, G.; Lunk, A. *Surf. Coat. Technol.* **2000**, *123*, 231.
(17) Huczko, A.; Lange, H.; Tyczkowski, J.; Kazimierski, P.; Tomassi, P. In *Electronic Properties of Novel Materials − Progress in Molecular Nanostructures*, XII International Winterschool, Kirchberg, Tyrol, Austria, March 1998; Kuzmany, H., Fink, J., Mehring, M., Roth, S., Eds.; AIP Conference Proceedings 544; American Institute of Physics: Woodbury, NY, 2000; p 230.
(18) Meubus, P.; Lange, H.; Jean, G. *Plasma Chem. Plasma Process.* **1989**, *9*, 527.
(19) Rao, C. N. R.; Sen, R.; Satishkumar, B. C.; Govindaraj, A. *Chem. Commun.* **1998**, *15*, 1525.
(20) Jones, J. M.; Malcolm, R. P.; Thomas, K. M.; Bottrell, S. H. *Carbon* **1996**, *34*, 231.
(21) Xia, Y.; Mu, Y.; Ma, Y.; Li, S.; Zhang, H.; Tan, C.; Mei, L. *Nucl. Instrum. Methods Phys. Res., Sect. B* **1999**, *155*, 395.